Effects of Negative Middle Ear Pressure on Wideband Acoustic Immittance in Normal-Hearing Adults

Sarah R. Robinson,[1] Suzanne Thompson,[2] and Jont B. Allen[1]

Objectives: Wideband acoustic immittance (WAI) measurements are capable of quantifying middle ear performance over a wide range of frequencies relevant to human hearing. Static pressure in the middle ear cavity affects sound transmission to the cochlea, but few datasets exist to quantify the relationship between middle ear transmission and the static pressure. In this study, WAI measurements of normal ears are analyzed in both negative middle ear pressure (NMEP) and ambient middle ear pressure (AMEP) conditions, with a focus on the effects of NMEP in individual ears.

Design: Eight subjects with normal middle ear function were trained to induce consistent NMEPs, quantified by the tympanic peak pressure (TPP) and WAI. The effects of NMEP on the wideband power absorbance level are analyzed for individual ears. Complex (magnitude and phase) WAI quantities at the tympanic membrane (TM) are studied by removing the delay due to the residual ear canal (REC) volume between the probe tip and the TM. WAI results are then analyzed using a simplified classical model of the middle ear.

Results: For the 8 ears presented here, NMEP has the largest and most significant effect across ears from 0.8 to 1.9 kHz, resulting in reduced power absorbance by the middle ear and cochlea. On average, NMEP causes a decrease in the power absorbance level for low- to mid-frequencies, and a small increase above about 4 kHz. The effects of NMEP on WAI quantities, including the absorbance level and TM impedance, vary considerably across ears. The complex WAI at the TM and fitted model parameters show that NMEP causes a decrease in the aggregate compliance at the TM. Estimated REC delays show little to no dependence on NMEP.

Conclusions: In agreement with previous results, these data show that the power absorbance level is most sensitive to NMEP around 1 kHz. The REC effect is removed from WAI measurements, allowing for direct estimation of complex WAI at the TM. These estimates show NMEP effects consistent with an increased stiffness in the middle ear, which could originate from the TM, tensor tympani, annular ligament, or other middle ear structures. Model results quantify this nonlinear, stiffness-related change in a systematic way, that is not dependent on averaging WAI results in frequency bands. Given the variability of pressure effects, likely related to intersubject variability at AMEP, TPP is not a strong predictor of change in WAI at the TM. More data and modeling will be needed to better quantify the relationship between NMEP, WAI, and middle ear transmission.

Key Words: Negative middle ear pressure, Power absorbance, Power reflectance, Wideband acoustic immittance.

(Ear & Hearing 2016;37;452–464)

INTRODUCTION

Wideband acoustic immittance (WAI) is a noninvasive diagnostic measurement for the middle ear, made over a range of speech frequencies relevant to human hearing (e.g., 0.2 to 8.0 kHz). The term WAI encompasses a large set of related quantities, including the complex (magnitude and phase) impedance, admittance, and reflectance, as well as power-based quantities (magnitude only) such as the power reflectance and absorbance level, all of which may be derived from ear-canal pressure measures in response to an acoustic stimulus (Møller 1960; Rabinowitz 1981; Allen 1986; Keefe et al. 1993; Voss & Allen 1994; Feeney et al. 2013). WAI is a proven tool for noninvasive differential diagnosis of middle ear pathologies in a clinical setting (Nakajima et al. 2012). Studies have shown systematic changes in the power reflectance for various pathological conditions of the middle ear, including disarticulation or fixation of middle ear joints, tympanic membrane (TM) perforations, or degrees of fluid in the middle ear cavity (Feeney et al. 2003; Allen et al. 2005; Shahnaz et al. 2009; Nakajima et al. 2012; Prieve et al. 2013). However, more analyses are required before WAI can reach its full clinical potential (Feeney et al. 2013). Here, a detailed analysis of the effects of negative middle ear pressure (NMEP) on WAI measurements in 8 individual ears is presented.

In the clinic, middle ear admittance is typically evaluated via tympanometry at 226 Hz, and the tympanic peak pressure (TPP) is used as an estimate of static middle ear pressure. Here, we investigate the relationship between TPP and changes in acoustic transmission in the middle ear, as characterized by the power absorbance level and complex WAI quantities estimated at the TM.

Wideband Acoustic Reflectance

The wideband complex acoustic reflectance, $\Gamma(f)$, is related to the admittance, $Y(f)$, by

$$\Gamma(f) = \frac{1 - r_0 Y(f)}{1 + r_0 Y(f)}. \quad (1)$$

The real quantity $r_0 = \rho_0 c / A_0$ is called the "surge resistance" (Robinson et al. 2013), where A_0 is the area of the ear canal, ρ_0 is the density of air, and c is the speed of sound.

WAI measurements are made with a Thévenin-calibrated probe sealed in the ear canal, containing at least one microphone and loudspeaker (Møller 1960; Allen 1986). A wideband acoustic stimulus, such as a steady-state periodic chirp, is played via the loudspeaker; the acoustic signal is partially reflected and partially absorbed, in a frequency-dependent manner, by the middle ear. The reflectance is defined as the complex ratio of the reflected to forward pressure (Keefe & Schairer 2011), as recorded by the probe microphone.

The "power reflectance," $|\Gamma(f)|^2$, is a measure of the relative fraction of the power reflected by the middle ear. A related quantity, the "power absorbance," $A(f) = 1 - |\Gamma(f)|^2$, measures the acoustic power absorbed by the middle ear and cochlea (Allen et al. 2005). The "power absorbance level" in decibels, plotted with a logarithmic frequency axis, has a very distinctive

[1]University of Illinois at Urbana-Champaign, Urbana, Illinois, USA; and [2]St. John's University, Queens, New York, USA.

<zdoi; 10.1097/AUD.0000000000000280>

shape for normal middle ears (Allen et al. 2005; Rosowski et al. 2012). Below about 1 kHz, normative data show a rising slope of 15 dB per decade (4.5 dB per octave). Above this breakpoint, the absorbance level is flat with a mean of −2 dB, and varies over a small decibel range (the ±1 standard deviation range is 2 to 3 dB in width). Rosowski et al. additionally characterize a falling slope of −23 dB per decade above 4 kHz. This band-pass response is qualitatively similar to estimates of the middle ear transfer function (Lynch et al. 1982; Puria & Allen 1991; Allen et al. 2005).

The reflectance phase, $\angle\Gamma(f)$, is a measure of signal latency. The "group delay," $\tau(f)$, which is defined as the negative slope of $\angle\Gamma(f)$ with respect to the radian frequency ($2\pi f$), is a frequency-dependent measure of round-trip signal delay in the ear canal and middle ear. Assuming a lossless ear canal of uniform area, the probe reflectance may be expressed as the product of the reflectance at the TM and a round-trip delay term, where the delay τ_{rec} is due to the residual ear canal (REC) length, L_{rec}, between the probe microphone and TM (Voss & Allen 1994). This gives

$$\Gamma(f) = \Gamma_{tm}(f) e^{-j2\pi f \tau_{rec}} \quad (2)$$

$$\angle\Gamma(f) = \angle\Gamma_{tm}(f) - 2\pi f \tau_{rec} \quad (3)$$

$$\tau(f) = \tau_{tm}(f) + \tau_{rec} \quad (4)$$

$$\tau_{rec} = 2L_{rec} / c. \quad (5)$$

For a REC of varying area (i.e., a human ear canal), the delay, τ_{rec} [Eq. (5)], can be a function of frequency, $\tau_{rec}(f)$ (Voss & Allen 1994).

Taking the magnitude of Equation (2) yields the result

$$|\Gamma(f)| \approx |\Gamma_{tm}(f)|, \quad (6)$$

since $\left|e^{-j2\pi f \tau_{rec}}\right| = 1$ in the ideal model of Equations (2)–(5). Equation (6) indicates that the reflectance magnitude approximately does not depend on probe depth in the ear canal. This is a reasonable assumption for adult ears (Voss & Allen 1994; Voss et al. 2008), which allows for comparisons across ears and probe insertion depths. Deviations from this relationship may increase with REC length due to the compliance of the ear canal tissue (Voss et al. 2008), particularly when the probe is seated outside of the bony portion of the ear canal. In many ears, canal compliance losses are relatively small compared with the variation across ears. Equation (6) is a standard assumption for WAI analysis, which typically considers only the power reflectance or absorbance level.

Effects of Middle Ear Pressure

Chronic NMEP is one of the most common middle ear pathologies (Shaver & Sun 2013). It typically occurs when the Eustachian tube is dysfunctional, such that the pressure behind the TM cannot be equalized to the ambient atmospheric pressure (Bluestone & Klein 2007). This pressure imbalance can cause a retraction of the eardrum, resulting in compression of the ossicular chain (Shaver & Sun 2013). It can result in a combination of NMEP and fluid in the middle ear cavity, and lead to chronic infections such as otitis media with effusion and bacterial biofilm (Bluestone & Klein 2007; Nguyen et al. 2012, 2013; Monroy et al. 2015).

Because NMEP is so common, a number of studies have considered its impact on otoacoustic emissions (OAEs), including transient evoked OAEs (Marshall et al. 1997; Prieve et al. 2008) and distortion product OAEs (DPOAEs; Sun & Shaver 2009; Thompson et al. 2015). As they require no behavioral response, OAE tests are widely used for infant hearing screening. However, middle ear pathologies such as middle ear fluid and NMEP confound the results of OAE tests, which depend on the round trip of a signal to and from the cochlea via the middle ear. Even small NMEPs less negative than −100 daPa, which are considered to be in the "normal" range, can compromise OAE test results (Sun & Shaver 2009).

The TPP naturally varies when the Eustachian tube is functioning normally. Typically it is negative during waking hours, and slightly positive when the subject is recumbent or sleeping (Tideholm et al. 1998). When a subject with normal middle ear function swallows or yawns the Eustachian tube briefly opens, causing a pressure equalization, leading to a time-varying TPP (on the order of minutes). This natural variation, or lack thereof, may be used to diagnose Eustachian tube dysfunction. By having subjects alter their middle ear pressure, using the Valsalva and Toynbee maneuvers,* the Eustachian tube function may be directly assessed (Holmquist & Olen 1980; Honjo et al. 1981). In the case of extreme dysfunction (e.g., otitis media with effusion), it is not possible to assess the middle ear pressure via tympanometry, due to extreme changes in the TM admittance resulting in no measurable TPP. As we will show, even in normal ears modest changes around zero TPP (e.g., −65 daPa) can produce easily observed changes in the WAI at the TM.

Two recent studies investigated the effects of static middle ear pressure on the power reflectance. Voss et al. (2012) showed there was a systematic increase in the power reflectance (decrease in the absorbance level) below 2 kHz as a function of static middle ear pressure in eight cadaver preparations with controlled MEPs over a ±300 daPa range. For individual ears, this increase was monotonic. Above 2.6 kHz, NMEP caused a decrease in the power reflectance (increase in the power absorbance level). Voss et al. modeled these acoustic changes using the network model of Kringlebotn (1988), assuming NMEP reduces the compliance of the TM and middle ear ligaments.

Similar results were obtained from 35 human subjects by Shaver and Sun (2013), who trained subjects to self-induce NMEPs. They reported averaged data from four NMEP ranges, but did not show data from individual ears. Shaver and Sun found that the power reflectance increased for low- to mid-frequencies and decreased above 3 kHz, with the largest changes occurring in the 1.0 to 1.5 kHz and 4.5 to 5.5 kHz ranges, respectively. They observed that the average magnitude of these changes increased with TPP magnitude. In addition, they used wideband tympanometry to compensate for NMEP, by measuring WAI while applying an equivalent pressure in the ear canal,

* The *Valsalva* maneuver induces a positive static middle ear pressure by forcibly exhaling with the mouth and nose closed; the *Toynbee* maneuver induces a negative static middle ear pressure by pinching the nostrils and swallowing.

which estimates WAI at the TPP. They found that, on average, compensating for the NMEP restored the power reflectance to near-baseline values. Considering the power reflectance results in Figures 1 and 3 of Shaver and Sun (2013), the average absorbance level would be about 2 dB higher at the compensated NMEP than at ambient middle ear pressure (AMEP) around 200 Hz, and about 0.5 dB higher around 1 kHz. Sun and Shaver (2009) also show that, averaged across ears, there is no significant difference between compensated-NMEP and AMEP measurements of DPOAEs. These studies show that average WAI measurements made at TPP and ambient ear-canal pressure are similar in normal ears.

For the measurements presented here, the probe was sealed in the ear canal at ambient atmospheric pressure. As in the Shaver and Sun (2013) study, subjects were trained to induce consistent TPP levels using the Toynbee maneuver (Thompson et al. 2015). Although it was not possible to simultaneously measure the TPP and WAI in the present study, the subjects were able to perform this task consistently and hold the NMEP for the duration of each test, as described in the "Materials and Methods" section.

Tympanometry

For the assessment of middle ear admittance, tympanometry is the clinical standard. In this procedure, the ear canal admittance, Y (related to the impedance by $Z = 1/Y$, and usually presented in milliliters), is measured at a single frequency, typically 226 Hz, using a probe that is hermetically sealed in the ear canal. This measurement is a function of static ear canal pressure, which is typically varied from +200 to −400 daPa.

Some fundamental assumptions of tympanometry are that (1) at 226 Hz the probe admittance is purely compliant (no friction losses), (2) it may be modeled as the sum of two compliances, $|Y_{\text{probe}}| \approx 2\pi f(C_{\text{me}} + C_{\text{rec}})$, where C_{rec} is proportional to the volume of the REC and C_{me} is the aggregate middle ear compliance at the TM, and (3) for extreme canal pressures C_{me} is zero (Shanks et al. 1988). Based on these three assumptions, the high pressure "tails" of the tympanogram are assumed to be equal to the REC compliance $C_{\text{rec}} \approx C_{\text{probe}}\big|_{+200\text{daPa}}$, which is subtracted from the probe compliance at TPP to obtain the compliance of the middle ear at the TM, $C_{\text{me}} = C_{\text{probe}}\big|_{\text{TPP}} - C_{\text{probe}}\big|_{+200\text{daPa}}$.

Assumption (3) has been questioned by several investigators (Rabinowitz 1981; Shanks & Lilly 1981; Shanks et al. 1988), who found that C_{me} is underestimated because it does not go to 0 at extreme pressures (thus the volume of the REC is overestimated). Rabinowitz models this error by relating changes in ear canal pressure to changes in hearing thresholds. Shanks and Lilly compare REC volumes estimated by tympanometry with measured volumes. They show that while both methods have errors larger than 20%, the negative tail of the tympanogram is a better estimator of REC volume than the positive tail.

Pressurizing the ear canal to eliminate the REC is a poor approximation above 500 or 600 Hz, because the admittance at the TM is not a simple compliance (assumption (2)). At higher frequencies, investigators using tympanometry typically consider the conductance "G" and susceptance "B" tympanograms, representing the real and imaginary parts of the complex admittance, respectively (Vanhuyse et al. 1975; Shanks et al. 1988).

Here, we relate WAI to tympanometry by directly estimating the REC volume and the equivalent compliance at the TM from the complex WAI. In this way, we define a relationship between WAI and three parameters derived from the tympanogram: TPP, peak compliance (or admittance), and REC volume. Using a published method (Robinson et al. 2013), we remove REC delay from WAI at all measured frequencies, approximating the WAI response at the TM.

MATERIALS AND METHODS

Subjects

Twenty-six adult subjects were recruited for the study, which was approved by the institutional review board of the City University of New York Graduate Center. All subjects had normal hearing and normal middle ear function, confirmed by a test battery including otoscopic examination, pure-tone threshold testing, tympanometry, and acoustic reflex testing. Subjects had little to no cerumen accumulation, healthy intact TMs, pure-tone air conduction thresholds below 15 dB HL (in octaves from 125 to 8000 Hz), normal 226 Hz tympanograms (GSI 33 Middle Ear Analyzer, Grason-Stadler), and acoustic reflex thresholds below 95 dB.

Out of the 26 subjects trained to induce consistent NMEP, 8 completed the study. NMEPs more negative than −50 daPa were desirable, as NMEPs in this range have been shown to affect middle ear transmission (Marshall et al. 1997; Prieve et al. 2008; Sun & Shaver 2009).

Data Collection

Subjects were trained to perform the Toynbee maneuver, in which NMEP is induced by pinching the nose while swallowing to completely block the passage of air, thus sucking air out of the middle ear cavity via the Eustachian tube. Tympanometry was used to assess subjects' ability to induce and maintain consistent NMEPs. A total of 16 admittance tympanograms were taken at 226 Hz for each subject at a sweep rate of −50 daPa/s, alternating eight trials at NMEP and eight trials at AMEP, such that each NMEP measurement was made from a separate attempt of the Toynbee maneuver. Subjects were instructed to swallow or yawn between trials to equalize the middle ear pressure. For each admittance tympanogram, the REC volume was estimated and removed based on the positive pressure tail at +200 daPa.

Figure 1 shows NMEPs induced by the 8 subjects over a −50 to −385 daPa range. Each box plot shows eight TPP measurements, collected from separate performances of the Toynbee maneuver, alternated with pressure equalizations. The measurements are divided into quartiles, with each median measurement shown as a horizontal line, the first and third quartiles as the bottom and top of a thin box, and outliers as circles. The gray box plots show the AMEPs, while the black box plots show the NMEPs. The subjects induced NMEPs with an average standard deviation of 22 daPa (individual standard deviations ranged from 2 to 39 daPa, excluding outliers). For all ears, the standard deviation was less than 25% of the mean NMEP magnitude (16% on average). As expected, there is little variation in the TPP values at AMEP, with an average standard deviation of 6 daPa (individual standard deviations ranged from 2 to 13 daPa).

WAI was measured during the same session using Mimosa Acoustics' HearID Middle Ear Power Analyzer (MEPA3). The system was calibrated according to the manufacturer's guidelines before collecting measurements. As in the tympanometry trials, eight trials each at AMEP and NMEP conditions were interleaved. During each trial, up to eight test–retest measurements were attempted, for a total of up to 64 measurements per

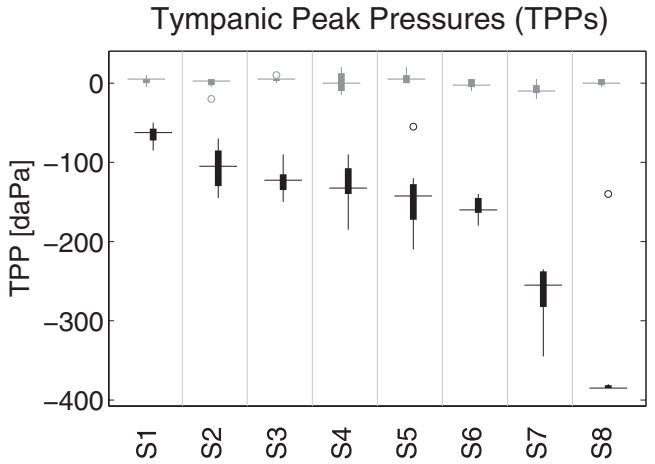

Fig. 1. Subjects were able to induce consistent NMEPs, estimated from the TPPs, using the Toynbee maneuver. Box plots show the measured TPPs at AMEP (*gray*) and NMEP (*black*) states. Each box plot divides the measurements into quartiles, showing the median measurement as a horizontal line, and the first and third quartiles as the bottom and top of the thin box. Outliers are shown as *circles*. TPPs are less variable in the AMEP state, as expected. All box plots show N = 8 trials, except for S6 and S8 (N = 7, NMEP), and S7 (N = 5, AMEP; N = 7, NMEP). AMEP, ambient middle ear pressure; NMEP, negative middle ear pressures; TPP, tympanic peak pressure.

pressure condition in each ear. Although WAI measurements typically have good signal to noise ratios, they can be affected, particularly at low frequencies, by mechanical noise in the environment or subject movements. This can be seen in the absorbance level curve below 500 Hz, where the absorbance is small. Because this frequency range is of interest for data analysis and modeling, WAI measurements presented here are chosen from sets of test–retest measurements to have the smoothest curves at low frequencies. The probe was not reinserted between trials, so the REC volume remained approximately constant for all measurements for a given subject.

These data were taken as part of a study designed to investigate the effects of middle ear pressure on DPOAE measurements (Thompson et al. 2015).

WAI Analysis

The complex TM reflectance, $\Gamma_{tm}(f)$, is estimated using a factorization method (Robinson et al. 2013) to remove variable delay due to the REC. This method separates the reflectance into TM and REC factors, $\Gamma(f) = \Gamma_{tm}(f)\Gamma_{rec}(f)$, after applying a parametric fitting procedure. The REC component, $\Gamma_{rec}(f) = e^{-j2\pi f \tau_{rec}(f)}$, accounts for lossless delay due to a REC of nonuniform area [Eqs. (2)–(5)]. From the REC delay, $\tau_{rec}(f)$ [Eq. (5)], we can estimate a frequency dependent canal length (Voss & Allen 1994). The remaining factor, $\Gamma_{tm}(f)$, defines the complex reflectance at the TM. Note that any lossless TM delay, as described by Puria and Allen (1998) and modeled by Parent and Allen (2010), may also be included in the REC component. The wideband TM admittance can be calculated using Equation (1), as $Y_{tm}(f) = (1/r_0)(1-\Gamma_{tm}(f))/(1+\Gamma_{tm}(f))$. This procedure extends assumptions (1) and (2) of tympanometry discussed in the "Introduction," avoiding the flawed assumption (3).

The reflectance factorization results allow us to determine the parameters of a simplified middle ear model shown in Figure 2A, consisting of a tube transmission line of length L_{rec} representing the REC, C_{me} representing the aggregate compliance of the middle ear at the TM, and a cochlear load resistance r_c, required to match the transmission lines of the middle ear and cochlea (Møller 1960; Zwislocki 1962; Lynch et al. 1982). The compliance C_{me} is nonlinear (represented by an arrow) since its value changes with NMEP. The model in Figure 2A qualitatively captures the behavior of the human middle ear up to 4 to 5 kHz. Due to its simplicity, the model cannot capture individual variations in the WAI above 600 Hz.

Figure 2B defines a low frequency (e.g., <600 Hz) network model for Figure 2A. The REC volume, V_{rec}, is related to the REC compliance by

$$V_{rec} = C_{rec}\rho_0 c^2, \tag{7}$$

where ρ_0 is the density of air and c is the speed of sound (Shanks et al. 1988). The reflectance factorization algorithm analyzes WAI for all frequencies, according to Figure 2A. For tympanometry, the input impedance of the middle ear is typically modeled by Figure 2B, at a single low frequency (e.g., 226 Hz), assuming $r_c = 0$. Adding a resistor to this model improves the fit to WAI data.

To relate the WAI results to the model, we first consider the complex TM impedance, $Z_{tm}(f) = 1/Y_{tm}(f)$, calculated via reflectance factorization. The TM impedance is considered, rather than the TM admittance, because its mathematical relationship to the model parameters is simpler. The TM impedance (due to C_{me} and r_c, with no REC component) is the same for both models in Figure 2,

$$Z_{tm}(f) = \frac{1}{Y_{tm}(f)} = R_{tm}(f) + jX_{tm}(f) \tag{8}$$

$$R_{tm}(f) = r_c \tag{9}$$

$$X_{tm}(f) = \frac{-1}{2\pi f C_{me}}, \tag{10}$$

where the resistance, $R_{tm}(f)$, and reactance, $X_{tm}(f)$, of the middle ear are related to the parameters r_c and C_{me}, respectively.

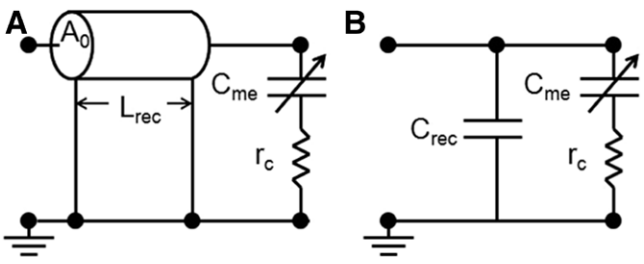

Fig. 2. A, A simplified wideband model of the REC and middle ear, showing the REC as a tube transmission line and the lumped middle ear compliance C_{me} and resistance r_c at the TM. This model qualitatively describes middle ear behavior up to about 4 or 5 kHz, capturing the general behavior of WAI but not individual variability. B, A low-frequency approximation of (A), where the tube transmission line is replaced by a compliance C_{rec} [proportional to the REC volume, Eq. (7)]. The resistor, r_c, is primarily due to the cochlear load, and is necessary to match the transmission lines of the middle ear and cochlea (Zwislocki 1962; Lynch et al. 1982). The compliance C_{me} is nonlinear (represented by an *arrow*) and changes with middle ear static pressure. REC, residual ear canal; TM, tympanic membrane; WAI, wideband acoustic immittance.

Thus, the model may be used to estimate C_{me}, and r_c from the low frequency WAI at the TM.

To estimate the REC compliance, C_{rec}, we must consider the reactance at the probe, $X(f)$, which is due to the REC and TM responses combined. Below 500 to 600 Hz, the compliances dominate the probe response and the reactance is modeled by

$$X(f) \approx \frac{-1}{2\pi f(C_{rec} + C_{me})}, \quad (11)$$

from which C_{rec} and subsequently V_{rec} may be estimated [Eq. (7)]. From WAI rather than a single-frequency measurement, frequency-dependent behavior such as that predicted by Equations (8)–(11) is easily modeled.

The reflectance factorization algorithm was experimentally verified by measuring the WAI for various volumes in a syringe. For each of two calibrated probe tips, 32 measurements were made, for a total of 64 measurements. The foam-tipped probe was sealed in the syringe, which was terminated by a rubber stopper attached to a plunger, and the volume was controlled by changing the plunger depth. Note that this termination, which is acoustically rigid, is expected to be different from the eardrum because it has no delay or acoustic loss. The syringe diameter was about 8.7 mm, slightly larger than the average diameter of the adult ear canal (about 7.5 mm). The rubber stopper had small conical peak, with a negligible volume of approximately 0.03 mL.

Figure 3 shows WAI estimates of the syringe volume made over a range of 0.2 to 1.7 mL, corresponding to a length range of about 3 to 29 mm. Some variability in the WAI estimates versus the measured lengths may be due to visual estimation of the syringe length, as the measured volumes appear to be quantized according to the volume markings on the syringe. A linear regression ($r^2 = 0.98$) shows that the volumes estimated via reflectance factorization are about 5% less than the measured volumes. This is likely due to acoustic losses in the syringe (Keefe 1984), as the reflectance factorization considers only lossless delay. Using the raw, unfiltered measurements (including losses), the regression line is $y = 0.98x + 0.06$ ($r^2 = 0.99$).

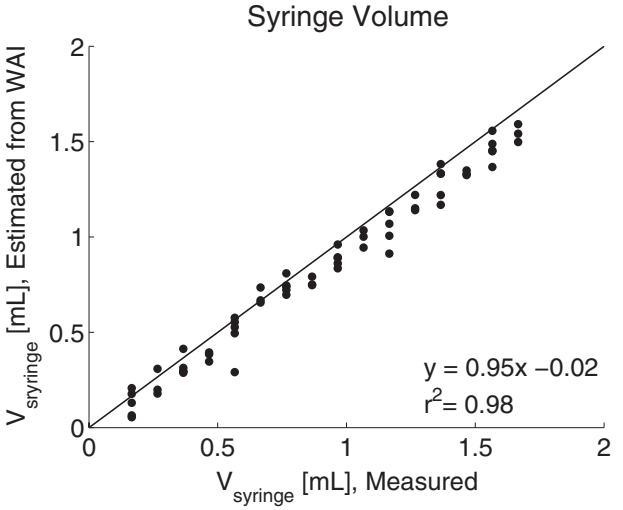

Fig. 3. Volumes in a syringe, estimated from WAI using the reflectance factorization method (Robinson et al. 2013). The volume range of 0.2 to 1.7 mL corresponds to a length range of about 3 to 29 mm. Variability in the measured lengths may be partially due to visual estimation of the syringe length, as the measured lengths appear to be quantized. Considering only the lossless delay, the volumes estimated from WAI are about 5% smaller than the measured volumes. WAI, wideband acoustic immittance.

RESULTS

Power Absorbance Level

Figure 4 shows absorbance level measurements in decibels for the 8 individual subjects, sorted by mean NMEP TPP (from Fig. 1, excluding outliers). Gray solid lines show the absorbance level for AMEP, while black dashed lines show it for NMEP. The light gray region shows normative data (±1 standard deviation) from Rosowski et al. (2012). For these 8 ears, the magnitude change in $A(f)$ with NMEP is 5 dB or less in most ears, although it is up to 10 dB for ear S8.

Most ears show a depression of the absorbance level due to NMEP for some range of frequencies below 2 kHz. This depression has a frequency range at least 1 kHz in width for all ears, and varies in size and location. The ears with the most severe NMEPs, S7 and S8, have the widest frequency ranges of separation between the pressure states, extending from at least 0.6 to 4.0 kHz. Above 2 to 3 kHz, the absorbance is generally similar between the AMEP and NMEP states. Half of the ears, S3, S5, S7, and S8, show a slight increase in absorbance level due to NMEP above 4 kHz, in agreement with the results of Shaver and Sun (2013) and Voss et al. (2012). For most ears, the absorbance level across trials in each pressure state remains fairly constant. Ear S3 shows the largest variation across measurements for a given pressure state, and the greatest overlap between the pressure states (particularly below 1 kHz). Ears S4 and S8 appear to have an intermediate pressure state, likely caused by inconsistencies in subjects' performance of the Toynbee maneuver.

The effects of NMEP may be grouped by similarity across ears. For the first group, ears S1, S2, and S7, NMEP change is characterized by a mid-frequency depression in the absorbance level beginning around 0.5 to 1.0 kHz. In Figure 4, we label these ears group A. The group B ears, S4, S5, and S8, show a large separation due to NMEP, extending all the way down to 0.2 kHz. For group B, NMEP appears to cause not only a depression of the absorbance level over this frequency range but also a systematic shift of its low frequency rising slope, upward in frequency. Ears S3 and S6 are less easily grouped. For ear S6, the NMEP curves are most separated from the AMEP curves from 0.8 to 1.5 kHz, but show slight separation of the states down to the lowest measurement frequencies. Ear S3 shows no absorbance level change below 1.5 kHz, but has a mid-frequency change due to NMEP around 2 kHz. Thus, ear S3 appears to be most similar to group A, while S6 seems most similar to group B (labeled (A) and (B)).

NMEP changes appear to be related to the baseline AMEP measurements. For example, ears S3 and S6 have noticeable small resonances (local minima and maxima) in the mid-frequency region from 1.0 to 4.0 kHz. This structure is altered by the NMEP in a systematic way; local resonances in the mid-frequency range become more pronounced, or shift upward in frequency due to the NMEP. Disparities in the effects of NMEP at low frequencies between groups A and B appear to be related to differences in the compliance (stiffness) characteristics of the middle ear, which dominate below 0.6 to 1.0 kHz. This is investigated in the following sections by considering the WAI at the

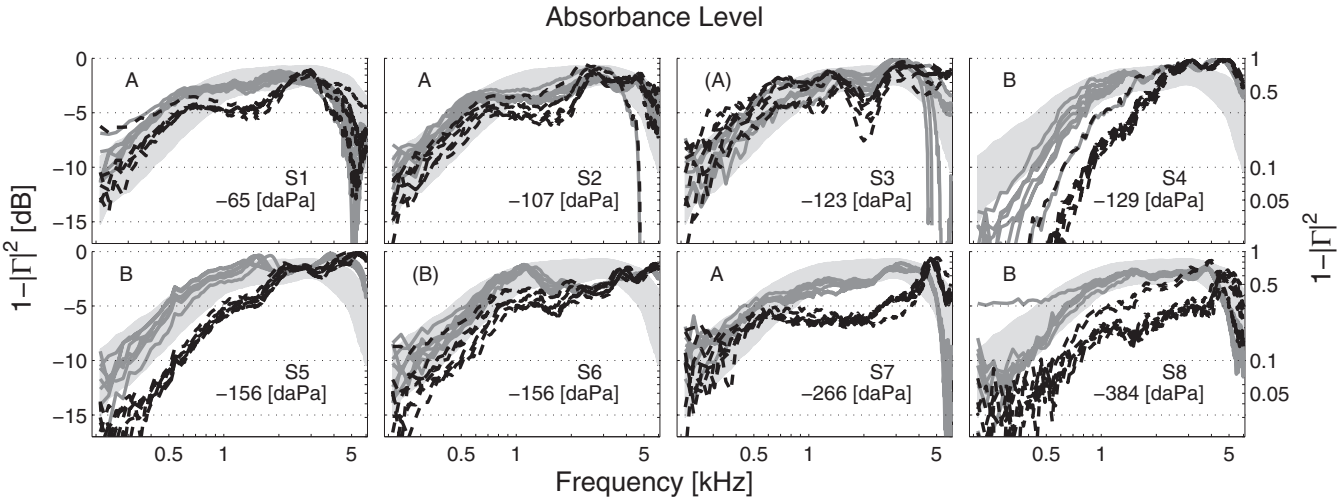

Fig. 4. Power absorbance level measurements at AMEP (*gray solid*) and NMEP (*black dashed*) for all ears, ordered by mean NMEP TPP. For each ear, N = 8 measurements are shown, selected to have the lowest noise from a pool of up to eight retest measurements [except for ear S1 (N = 6, AMEP and NMEP), ear S2 (N = 7, NMEP), and ear S7 (N = 7, AMEP)]. For the majority of the ears, there is a decrease in the absorbance level below 2 kHz due to NMEP, and a small increase above 4 to 5 kHz. The *light gray* region shows ±1 standard deviation for normative data from Rosowski et al. (2012). AMEP, ambient middle ear pressure; NMEP, negative middle ear pressure; TPP, tympanic peak pressure.

TM, which shows that the group B ears experience a greater decrease in the compliance at the TM due to NMEP.

Figure 5 summarizes the results across ears, as compared with the study of normal ears by Rosowski et al. (2012). Normative data from Rosowski et al. are displayed using a solid line for the mean curve and error bars showing ±1 standard deviation. Mean curves for the current experiment are shown as dashed lines for the AMEP (open circles) and NMEP (solid squares) states, along with regions of ±1 standard deviation (light gray and dark gray, respectively, and medium gray where the regions overlap). Mean and standard deviation calculations were weighted to favor each ear equally. The AMEP distribution from this study shows excellent agreement with normative data from Rosowski et al., as the mean AMEP curve is within 1 dB of the Rosowski et al. mean for all measured frequencies. Mean curves show a decrease in the absorbance level for low- to mid-frequencies due to NMEP, and an increase above about 4 kHz.

Using the eight individual mean curves at both AMEP and NMEP, significance testing was performed at each frequency point. Considering the NMEP change relative to baseline AMEP measurements (using a paired *t* test), the absorbance level was significantly lower at NMEP from 0.4 to 2.0 kHz ($p < 0.01$), and higher from 4.5 to 6.0 kHz ($p < 0.05$). Considering the overall separation of NMEP and AMEP results (using an unpaired *t* test), the absorbance level was significantly lower from 0.6 to 2.0 kHz ($p < 0.01$), and the most significant separation occurred from 0.8 to 1.9 kHz ($p < 0.002$; $p < 10^{-15}$ using all data in Fig. 5). In Figure 5, there is almost no overlap of the ±1 standard deviation regions in the 0.8 to 1.9 kHz range, where the separation between mean AMEP and NMEP curves is 2 dB on average.

Residual Ear Canal Contributions to WAI

REC delays, $\tau_{rec}(f)$ [Eq. (4)], due to the space between the probe and the TM are shown in Figure 6, ordered by mean NMEP TPP. These frequency-dependent delays were calculated as described in the "Materials and Methods" section. AMEP and NMEP states are shown as gray solid and black dashed lines, respectively. These responses are smooth due to the parametric fit to the complex reflectance, $\Gamma(f)$, from which $\Gamma_{rec}(f)$ and subsequently $\tau_{rec}(f)$ are derived.

Although probe insertions were not intentionally modified between measurements, a few ears show changes in $\tau_{rec}(f)$ that are independent of pressure state. For example, ear S1 (top left plot) shows a varying $\tau_{rec}(f)$ function across measurements, meaning the estimated REC length changed during data collection. The largest change in $\tau_{rec}(f)$ for S1 occurred between 2 and 3 kHz, where there is a peak in $\tau_{rec}(f)$ that changed with time.

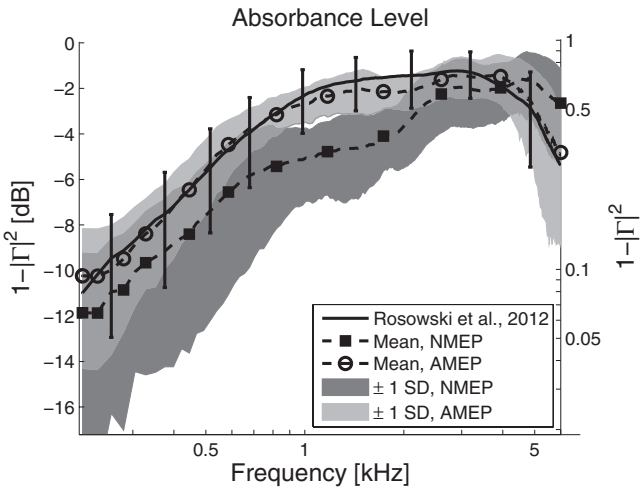

Fig. 5. Absorbance level distributions showing ±1 standard deviation for the AMEP (*light gray*, N = 61) and NMEP (*dark gray*, N = 61) states (*medium gray* indicates where the standard deviation regions overlap). Mean curves for each state are shown as *dashed lines* (AMEP, *open circles*; NMEP, *solid squares*). Mean and variance calculations were weighted to favor all ears equally. Normative data from Rosowski et al. (2012) are shown as a *solid line* (mean curve) with error bars showing ±1 standard deviation (N = 58). The AMEP mean from this study is in close agreement with the Rosowski et al. normal mean. AMEP, ambient middle ear pressure; NMEP, negative middle ear pressure.

The TM delay, $\tau_{tm}(f)$, and the total delay, $\tau(f)$, are also shown for ear S1 in Figure 7. When the REC delay is removed from the total delay (left), the resulting TM delay, $\tau_{tm}(f) = \tau(f) - \tau_{rec}(f)$ (right), is more coherent across trials. The variation in $\tau_{tm}(f)$ is slightly greater in the AMEP state, consistent with variation of the absorbance level curves in Figure 4.

Estimated WAI at the TM

Figures 8, 9, and 10 show the estimated complex TM impedance, $Z_{tm}(f) = R_{tm}(f) + jX_{tm}(f)$ [Eqs. (8)–(10)]. Specifically, the resistance, $R_{tm}(f)$, reactance, $X_{tm}(f)$, and magnitude impedance, $|Z_{tm}(f)|$, are shown. Consistent with the absorbance level results in Figure 4, these TM impedance estimates show systematic separation of the AMEP and NMEP states.

Figures 8 and 9 give the estimated wideband TM resistance and reactance for each of the eight ears. As in Figure 4, the results are ordered by mean NMEP TPP, for the AMEP (gray solid) and NMEP (black dashed) states. From Equation (9), the resistance is expected to be approximately independent of frequency. For most of the ears in Figure 8, the resistance remains between two and six times the surge resistance, r_0, of the ear canal (by which the impedance is normalized), especially in the AMEP state. While the TM resistance changes with NMEP for some range of frequencies in all ears, the largest change in R_{tm} occurs in ears S7 and S8, which had the largest NMEPs. The reactance curves in Figure 9 all have a $1/f$ dependence up to at least 500 or 600 Hz, as predicted by Equations (8)–(10). The NMEP measurements fall below the AMEP measurements, corresponding to a decreased aggregate compliance at the TM [C_{me}, Eq. (10)]. Ears S4, S5, and S8 (group B) show the largest separation of pressure states at low frequencies, indicating the largest decrease in middle ear compliance due to NMEP.

Note that at very low frequencies below 400 Hz, the resistance can be an order of magnitude smaller than the reactance, resulting in unreliable estimates of the TM resistance (Fig. 8). Although the low frequency TM resistance curves appear smooth, due to the parametric fitting procedure, large variations (e.g., S1, S7, S8) can occur due to measurement noise, as described in the "Materials and Methods" section. For example, the NMEP data for S8 in Figure 4 (bottom right) appear to be very noisy (jagged) at low frequencies below 400 Hz. Considering Figure 9, the normalized TM reactance for this ear is very large (less than –20) below 500 Hz. Thus, the corresponding TM resistance curves (of much smaller normalized magnitudes) have a wide range of values at low frequencies, including nonphysical negative values.

Figure 10 gives the estimated wideband TM impedance magnitudes in the style of Figures 8 and 9. Below about 0.5 to 1.0 kHz, $|Z_{tm}(f)|$ is dominated by the compliance at the TM ($|Z_{tm}| \approx |X_{tm}| \approx 1/(2\pi f C_{me})$), which appears as a straight line with a negative slope of 1 on a log–log scale. In the mid-frequency range where the TM reactance (Fig. 9) becomes small, the TM resistance (Fig. 8) dominates.

Comparing Figures 8, 9, and 10, the largest systematic effect of NMEP is a decreased compliance (increased stiffness) at the TM, characterized by a low frequency decrease in $X_{tm}(f)$ and increase in $|Z_{tm}(f)|$. NMEP also appears to shift various local middle ear resonances, as in Figure 4. For example, ear S5 has a small (about 3 dB) minimum in the TM impedance magnitude at AMEP at 1.5 kHz (Fig. 10, bottom left). In the NMEP state, this local minimum shifts to 2.5 kHz, corresponding to a similar shift observed in the NMEP absorbance level (Fig. 4, bottom left).

Model Parameters

The REC volumes, V_{rec}, and middle ear compliances, C_{me}, estimated from the WAI data are given in Figure 11. The model described by Figure 2B [Eqs. (8)–(11)] was fit to the complex TM impedance, $Z_{tm}(f)$, below 500 Hz (mean fit error was less than 10% for over 90% of the measurements). AMEP and NMEP results are displayed as gray and black boxplots, respectively. Figure 11A shows the REC volumes [Eq. (7)], ordered by mean NMEP TPP. These volumes are significantly different ($p < 0.05$ using an unpaired t test) between the AMEP and NMEP states for ears S3, S4, and S5. The change in median REC volume due to NMEP ranges from 0.01 to 0.18 mL. Corresponding REC lengths (assuming a constant ear canal area) are given on the right-side axis.

Figure 11B shows the estimated middle ear compliances, C_{me}, ordered by mean NMEP TPP. These values are given in milliliters [calculated using Eq. (7)], which allows for comparison to

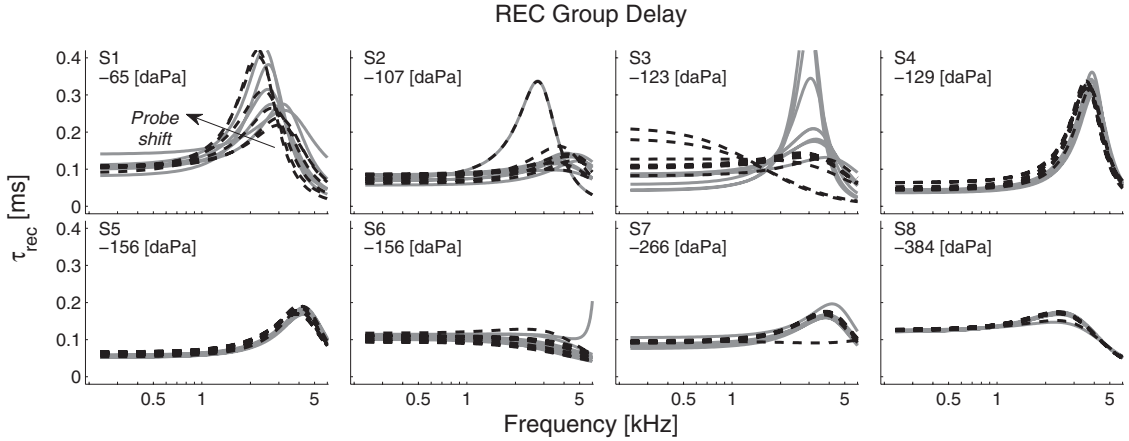

Fig. 6. The estimated REC group delay, $\tau_{rec}(f)$ [Eq. (4)], is shown for all ears. AMEP (*gray solid*) and NMEP (*black dashed*) states are shown, ordered by mean NMEP TPP. Note that these responses are smooth due to the parametric fit to the complex reflectance, $\Gamma(f)$, from which $\tau_{rec}(f)$ is derived. Some ears, particularly ear S1, show differing responses across measurements which do not depend on the pressure state. This is likely due to changes in the probe insertion. AMEP, ambient middle ear pressure; NMEP, negative middle ear pressure; REC, residual ear canal; TPP, tympanic peak pressure.

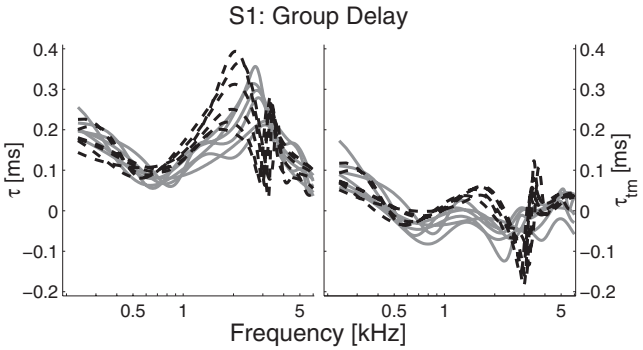

Fig. 7. The total group delay, $\tau(f)$, and TM group delay, $\tau_{tm}(f)$, for subject S1. AMEP (*gray solid*) and NMEP (*black dashed*) states are shown. Removing the group delay due to the REC, $\tau_{tm}(f) = \tau(f) - \tau_{rec}(f)$, visibly reduces variability in $\tau_{tm}(f)$ with respect to $\tau(f)$. Note that these responses are smooth due to the parametric fit to the complex reflectance, $\Gamma(f)$, from which $\tau(f)$ and $\tau_{tm}(f)$ are derived. AMEP, ambient middle ear pressure; NMEP, negative middle ear pressure; REC, residual ear canal; TM, tympanic membrane.

tympanometry, and direct comparison of V_{rec} and C_{me} magnitudes. The middle ear compliance values at the TM are significantly lower in the NMEP state ($p < 0.01$, using an unpaired t test), except for ear S3. The change in median C_{me} due to NMEP ranges from 0.21 to 1.34 mL (not including S3). Ear S3 has a wide spread of C_{me} and V_{rec} values, likely due to measurement variation and noise, visible in the absorbance curves of Figure 4. The group B ears (S4, S5, S8), which showed greater separation at low frequencies due to NMEP in Figures 4, 9, and 10, have larger changes in C_{me} than the group A ears. Median r_c values (not shown) at AMEP are between 1.8 and 4.3 times the surge resistance, r_0, except for S4. These values are significantly different in the NMEP state only for ears S4 and S7 ($p < 0.01$).

Figure 12 shows peak compensated static acoustic admittance values estimated via tympanometry at 226 Hz, $|Y_{tm}|_{f=226\text{Hz}}$, compared with $|Y_{tm}|_{f=226\text{Hz}}$ values estimated using WAI at AMEP. WAI estimates include AMEP C_{me} values given in Figure 11B, along with r_c values (not shown), according to the model in Figure 2B. Boxplots of $|Y_{tm}|_{f=226\text{Hz}}$ are shown for WAI (gray) and tympanometry (black). Note that the tympanometric measurements were rounded to the nearest 0.1 mL by the measurement device; this quantization can be seen in the boxplots. Tympanometric estimates of $|Y_{tm}|_{f=226\text{Hz}}$ are significantly lower than WAI estimates for all ears except S3 and S8. The variability is similar for both methods of estimating the 226 Hz TM admittance, although slightly higher for the WAI measurements. Average standard deviations are 0.10 and 0.08 for WAI and tympanometry, respectively (excluding outliers).

DISCUSSION

Dependence of WAI Changes on NMEP

General changes in the power absorbance level with NMEP, characterized by a depression below about 2 kHz followed by a small elevation at higher frequencies, as seen in Figures 4 and 5, are consistent with the results of Voss et al. (2012) and Shaver and Sun (2013). Figure 5, which shows the means and standard deviation regions for the AMEP and NMEP absorbance level measurements across ears, indicates that the mid-frequency region from 0.8 to 1.9 kHz is optimal for detecting NMEP in these ears, as shown in the "Results" section. This is in agreement with the results of Shaver and Sun who found that the largest change in the power reflectance occurred from 1.0 to 1.5 kHz. Based on this observation, for each of the 8 ears, we averaged the absorbance level from 0.8 to 1.9 kHz to explore its relationship to TPP, as shown in Figure 13. Outliers from Figure 1 and suspected intermediate pressure states from Figure 4 (S4 and S8) are excluded in this analysis. A TPP more negative than −50 daPa causes a decrease in the mean 0.8 to 1.9 kHz absorbance level for all ears, except S3. There is a significant linear regression of these quantities ($r^2 = 0.79$, $p < 0.001$). However, a quadratic regression provides a similar fit ($r^2 = 0.81$, $p < 0.001$), implying that the relationship between power absorbance level and TPP may be nonlinear.

Although Figure 13 yields a significant relationship between TPP and WAI for these 8 ears, investigators should be careful when averaging data in frequency bins. Considering the absorbance level measurements of Figure 4, the frequency ranges and magnitudes of NMEP effects vary across ears. For

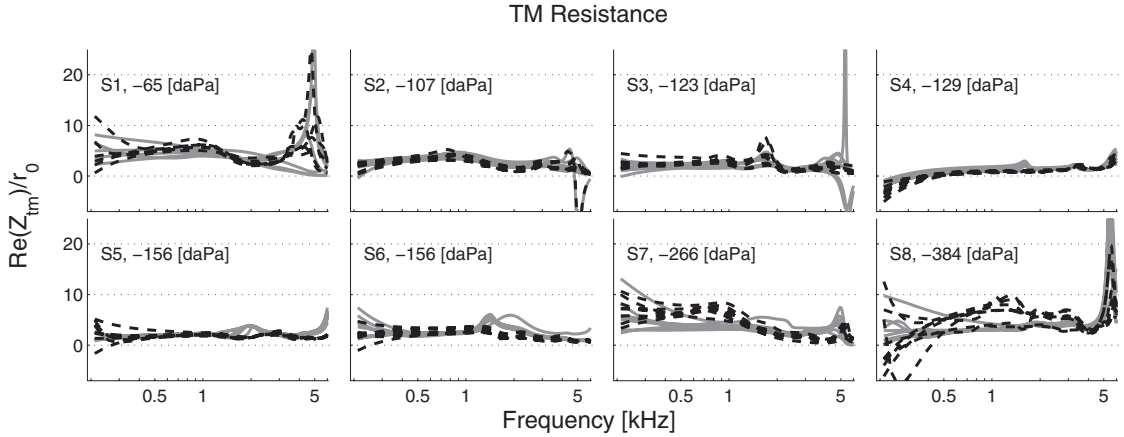

Fig. 8. Wideband TM resistance estimates, $R_{tm}(f)$ (the real part of the TM impedance, $Z_{tm}(f)$). AMEP (*gray solid*) and NMEP (*black dashed*) states are shown for all ears, ordered by mean NMEP TPP. These curves are normalized by the ear canal surge resistance, r_0, defined for Equation (1). For most of the ears, the resistance remains between 2 and 6 normalized units. These data are smoothed at all frequencies by the parametric fitting procedure; low frequency variability below 400 Hz may be due to measurement noise and to the large disparity in magnitude between the TM resistance and reactance. AMEP, ambient middle ear pressure; NMEP, negative middle ear pressure; TM, tympanic membrane; TPP, tympanic peak pressure.

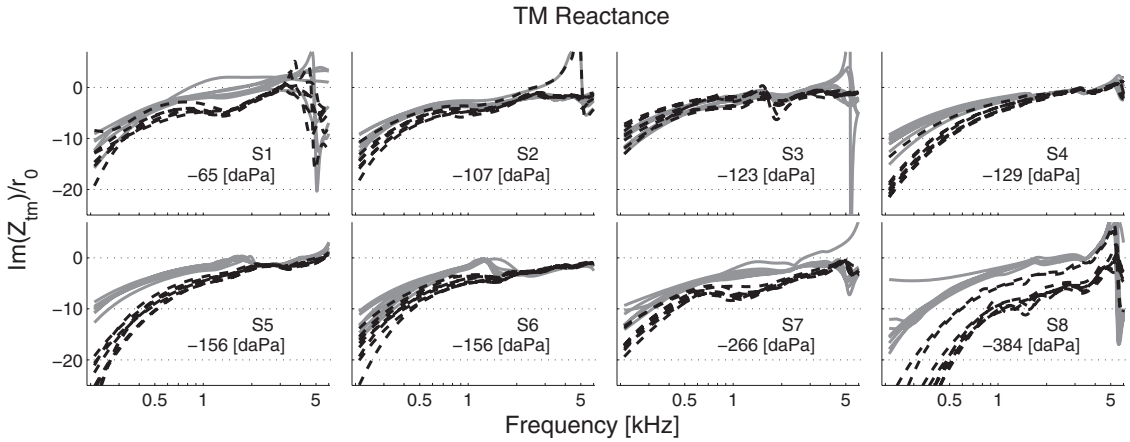

Fig. 9. Wideband TM reactance estimates, $X_{tm}(f)$ (the imaginary part of the impedance, $Z_{tm}(f)$). AMEP (*gray solid*) and NMEP (*black dashed*) states are shown for all ears, ordered by mean NMEP TPP. These curves are normalized by the ear canal surge resistance, r_0 [Eq. (1)]. The low frequency reactance has a $1/f$ dependence, as predicted by Equation (10). NMEP causes an increase in the TM reactance magnitude [decrease in C_{me}, Eq. (10)] below 2 to 4 kHz for most ears. AMEP, ambient middle ear pressure; NMEP, negative middle ear pressure; TM, tympanic membrane; TPP, tympanic peak pressure.

instance, in ear S3, NMEP causes a mean depression of the absorbance level of about −2 dB at 2 kHz. Although this is a similar magnitude change to those observed for the other ears, it occurs outside of the 0.8 to 1.9 kHz frequency range over which the absorbance was averaged. Also consider ears S5 and S6, which have similar NMEP TPPs but show disparate NMEP effects at low frequencies (this is true of S3 and S4 as well). Increased stiffness of the middle ear due to NMEP shifts features of the absorbance level (such as the low frequency rising slope, and local resonances) upward in frequency, but this effect varies due to intersubject variability at AMEP. Thus, the 0.8 to 1.9 kHz region merely contains the most overlap of NMEP changes across ears. Alternatively, fitting these data to a parametric model can be a more meaningful approach to characterize WAI change.

Changes in WAI at the TM with NMEP are consistent with increased stiffness (decreased compliance) in the middle ear. This is seen in the TM reactance and magnitude impedance responses in Figures 9 and 10, as a separation of the AMEP and NMEP states at low frequencies, and shifts in the mid-frequency local resonances. The decrease in compliance due to NMEP is captured by the model parameter C_{me} in Figure 11B. The group B ears (S4, S5, S8) show the largest changes in C_{me}, but did not all have the largest pressures. It is likely that the level of change in C_{me} is related to intersubject variability at AMEP. For instance, the middle ear cavity volume contributes to the compliance at the TM and could be a source of variability across subjects below 2 kHz (Voss et al. 2008, 2013), which could affect the NMEP-related change in C_{me}. Intersubject variability may also be due to differences in the nonlinear compliance characteristics of the TM and ossicular chain.

Removal of the Residual Ear Canal Effect

Considering Figures 6 and 11A, the frequency-dependent REC delays, $\tau_{rec}(f)$, and the estimated volumes, V_{rec}, are relatively constant across pressure conditions and retest measurements for most ears. For 6 of the ears, V_{rec} is estimated to be slightly larger in the NMEP condition. This could be due to systematic shifts of the probe during the Toynbee maneuver, or to

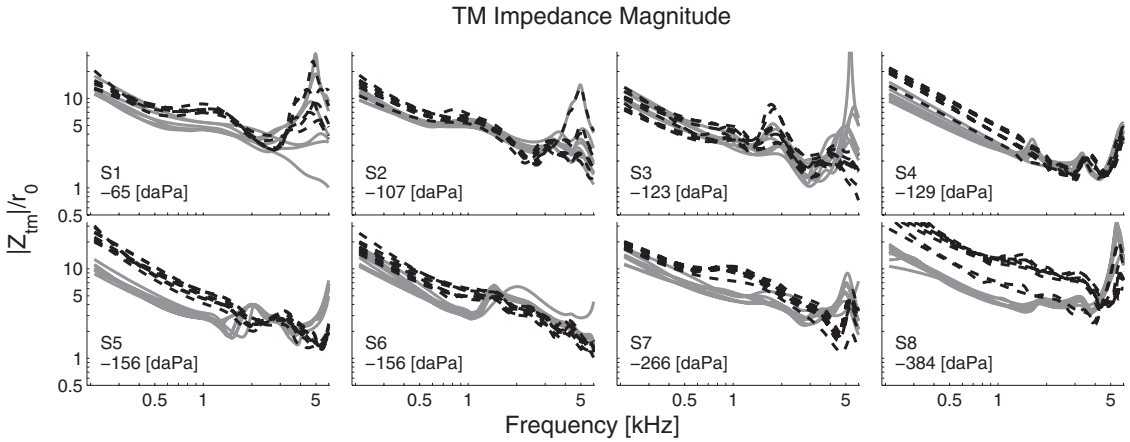

Fig. 10. Estimated wideband TM impedance magnitudes, $|Z_{tm}(f)|$. AMEP (*gray solid*) and NMEP (*black dashed*) states are shown for all ears, ordered by mean NMEP TPP. These curves are normalized by the ear canal surge resistance, r_0 [Eq. (1)]. $|Z_{tm}(f)|$ is dominated by the reactance, $X_{tm}(f)$ (Fig. 9), at low frequencies, and by the resistance, $R_{tm}(f)$ (Fig. 8), at mid-frequencies, where $X_{tm}(f)$ is small. AMEP, ambient middle ear pressure; NMEP, negative middle ear pressure; TM, tympanic membrane; TPP, tympanic peak pressure.

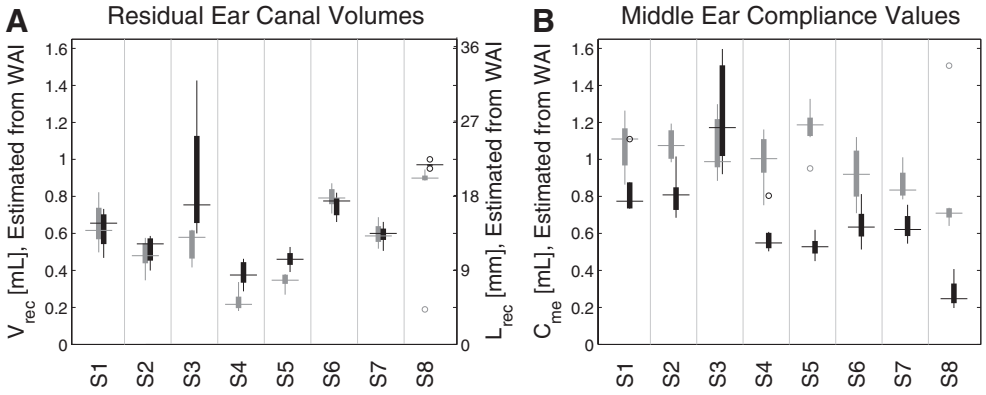

Fig. 11. A, REC volumes estimated via reflectance factorization, proportional to C_{rec} [Eq. (7)]. The right-side axis gives the corresponding estimated REC lengths, assuming a uniform ear canal area. B, Lumped middle ear compliances C_{me} at the TM, estimated from the TM impedance, $Z_{tm}(f)$ [Eqs. (8)–(10)]. These values are given in milliliters [via Eq. (7)] for easy comparison with the V_{rec} values and tympanometry. Black box plots show the NMEP results, and gray box plots show the AMEP results, ordered by mean NMEP TPP. For all ears (other than the high variance subject S3) the TM compliance, C_{me}, is significantly lower in the NMEP state ($p < 0.01$), and for most ears the V_{rec} estimates show an insignificant or relatively small change between the pressure states. AMEP, ambient middle ear pressure; NMEP, negative middle ear pressure; REC, residual ear canal; TM, tympanic membrane; TPP, tympanic peak pressure.

displacement of the TM due to NMEP. Changes in V_{rec} are small compared with the changes in C_{me} with NMEP (ranging from 6% to 35% of the C_{me} change, except for S3).

As shown in Figure 6, some ears show changes in $\tau_{rec}(f)$ that are independent of pressure state, which may indicate "drift" in the probe insertion. Such drifts could be caused by small movements of a subject's head between measurements, or the weight of the cable slowly pulling the probe out of the ear canal. Considering $\tau_{rec}(f)$ for subject S1 (top left plot), the REC group delay changed systematically with time during data collection, showing an increasing mid-frequency peak. Such a peak is functionally consistent with an area constriction in the REC (Karal 1953; Puria 1991), which could be due to the angle of the probe in the ear canal (e.g., a drooping probe insertion). Considering Figure 7, removing the time-varying REC delay gives a more consistent estimate of the complex WAI at the TM, which shows that the reflectance factorization can be highly effective.

TM Admittance at 226 Hz: WAI Versus Tympanometry

Figure 12 shows that the 226 Hz TM admittance is consistently lower when estimated via tympanometry, compared with WAI. As studied by Rabinowitz (1981) and Shanks and Lilly (1981), our results show that it is incorrect to assume that the compliance at the TM is zero at static ear-canal pressure extremes, such as +200 daPa (assumption (3) of tympanometry, as described in the "Introduction"). This assumption causes the admittance (compliance) at the TM to be underestimated. In Figure 12, mean tympanometric estimates are 7% to 46% lower than mean WAI estimates (excluding outliers),

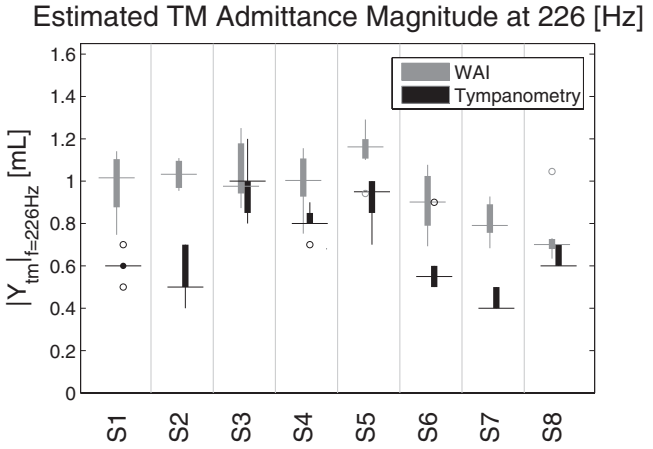

Fig. 12. Comparison of mean 226 Hz TM admittance magnitude values, $|Y_{tm}|_{f=226Hz}$, estimated by tympanometry (*black box plots*) with those estimated from WAI (*gray box plots*) at AMEP. The tympanometric estimates are significantly lower than the WAI estimates for all ears except S3 and S8 ($p < 0.005$). On average, tympanometry underestimates the TM compliance by 27%, as previously observed (Rabinowitz 1981; Shanks & Lilly 1981). AMEP, ambient middle ear pressure; TM, tympanic membrane; WAI, wideband acoustic immittance.

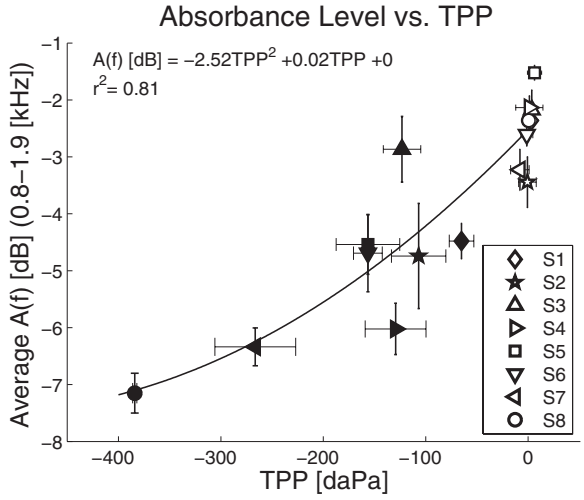

Fig. 13. Mean power absorbance level over the 0.8 to 1.9 kHz range as a function of mean TPP. Error bars show ±1 standard deviation for each quantity (excluding outliers). AMEP data are shown as *open symbols*, and NMEP data are shown as *filled symbols*. There is a significant quadratic regression ($r^2 = 0.81$, $p < 0.001$). As expected, the AMEP data are clustered around 0 daPa; note that the symbols for ears S1 and S3 are hidden by those for ears S4, S6, and S8. AMEP, ambient middle ear pressure; NMEP, negative middle ear pressure; TPP, tympanic peak pressure.

27% lower on average, in agreement with Rabinowitz. The variation in these errors is most likely related to individual characteristics of the TM and middle ear when the ear-canal pressure is +200 daPa.

Part of the error in the tympanometric estimates of the 226 Hz TM admittance is due to the fact that these estimates are typically lower when the positive tympanogram tail is used to compensate for the REC volume (Shanks & Lilly 1981). Shanks and Lilly showed that the error in REC volume estimated at 220 Hz was 39% using the positive tail, and 24% using the negative tail. However, in this study, it was prudent to compensate for the REC using the positive tail, because negative shifts in the TPP due to NMEP could artificially raise the compliance of the negative tail.

Although these results indicate that the tympanometric errors in $|Y_{tm}|_{f=226\text{Hz}}$ are significant, their clinical relevance is tied to the current utility of the peak compensated static acoustic admittance parameter. In tympanometry, peak compensated admittance is a measure of middle ear compliance, as the admittance at the TM is dominated by stiffness characteristics at 226 Hz (Figs. 2, 8, and 9). Low compliance (high stiffness) is linked to middle ear pathologies, such as middle ear effusion, otosclerosis, thickened TM, and malleus fixation (Shanks & Shohet 2009). Therefore, if the estimated value of $|Y_{tm}|_{f=226\text{Hz}}$ is too low, it could lead to a false positive diagnosis indicating one of these disorders.

According to Shanks and Shohet (2009), the clinical utility of the peak compensated admittance is questionable, due to high normal variability and significant overlap between $|Y_{tm}|_{f=226\text{Hz}}$ distributions for normal and pathological middle ears. They hypothesize that some of this variability is related to inconsistent compensation methods (e.g., whether the positive or negative tympanogram tail is subtracted from the peak). Further variability is due to the fact that the compliance at the TM does not go to zero at static pressure extremes. Instead, individual ears have varying TM compliance characteristics at the pressure extremes used in tympanometry. It is likely that the error in $|Y_{tm}|_{f=226\text{Hz}}$ as estimated via tympanometry is one of the primary reasons why the parameter is not clinically useful.

Mechanisms for Pressure-Dependent Changes in WAI

As discussed with regard to Figures 4, 10, and 11B, the effect of NMEP on WAI may be primarily described as an increased stiffness in the middle ear system, characterized by C_{me} (Fig. 2). A NMEP-dependent stiffness measured at the TM could be due to many middle ear structures including the TM, ossicle joints, muscles, and ligaments (Voss et al. 2012). However, it is not fully understood which middle ear structures contribute to WAI changes due to NMEP, and to what extent. It is commonly assumed that the TM is the largest contributor to nonlinear, NMEP-dependent stiffness characteristics in such data. For example, in assumption (3) of tympanometry it is often stated that the TM itself becomes stiff when pressurized. However, it has been shown that the TM functions primarily as a delay line (Puria & Allen 1998). Thus, it is more likely that the nonlinear NMEP effect is primarily due to the middle ear ligaments, particularly when the NMEP is within the range of normal variation (Pang & Peake 1986).

Retraction of the TM due to NMEP is likely similar to TM displacement due to contraction of the tensor tympani muscle. Unlike the stapedius muscle, the tensor tympani is not activated as part of the acoustic reflex in humans (Møller 1983), thus, how it functions, what causes it to contract, and its effects on the acoustic impedance are not well understood (Mukerji et al. 2010; Aron et al. 2015). Studies in cats, rabbits (Møller 1983), and humans (Bance et al. 2013; Aron et al. 2015) indicate that the effect of tensor tympani contraction on WAI would be similar to that of stapedius muscle contraction. In vivo measurements in human ears of the acoustic stapedius reflex, which applies a force on the annular ligament, increasing its stiffness and changing the motion of the stapes footplate (Møller 1983), show similar changes in WAI to those found here (Feeney & Keefe 1999; Feeney et al. 2004; Schairer et al. 2007). Thus, it seems likely that NMEP is acting on the annular ligament, tensor tympani, or both.

Nonlinear characteristics of the annular ligament have been previously measured and modeled (Lynch et al. 1982; Pang & Peake 1986; Murakami et al. 1997; Lauxmann et al. 2014). The effects of NMEP on WAI found here are consistent with changes in the stapes response due to a pressure differential across the annular ligament (Lynch et al. 1982; Lauxmann et al. 2014). According to measurements of Lynch et al. in cat, a partial middle ear system consisting of the stapes, annular ligament, and cochlea gives an impedance change due to static pressure (in the cavity around the stapes) that is similar to the impedance changes observed in Figure 10. In human cadaver ears, Murakami et al. found a decrease in stapes (as well as umbo) vibration at low frequencies (related to an increase in impedance, as in Fig. 10), and an increase at high frequencies, given a decrease in middle ear pressure. The same research team also found a decrease in stapes velocity at low frequencies when the pressure in the cochlea was increased instead (Myers et al. 1998).

The overall shift in TM impedance due to an increased stiffness, seen here as an increase in the impedance below 1 to 2 kHz, followed by a small decrease in impedance at high frequencies (for some ears), is described via a simple resonance by Feeney and Keefe (1999). The term resonance is typically defined by a second order system, such as series capacitor–inductor system, modeling a stiffness and mass (e.g., a simple harmonic oscillator). The so-called middle ear resonance is better characterized as a resistor in series with a capacitor, namely, the first order system described by Figure 2A.

As noted in the "Results" section, the resistance at the TM, modeled by r_c, depends on NMEP for some frequencies, particularly at large NMEPs. These changes are related to power dissipation in the middle ear, which could be due to a compression of the ossicle joints. This effect is most severe for ears S7 and S8, which have the largest NMEP TPP values.

Clinical Implications

For clinicians and investigators working with WAI, it is important to understand how a wide range of pathologies, including NMEP, may affect their measurements. Here, we see a systematic stiffness change due to NMEP, which is similar to that due to otosclerosis or the acoustic stapedius reflex. Understanding the particular effects of NMEP on WAI can aid in better differential diagnoses of similar pathologies. Our results indicate that TPP is not a reliable predictor of immittance changes at the TM over a broad range of frequencies (Figs. 4

and 13). Future modeling of individual variations in these measurements, due to the stiffness of the middle ear ligaments and volume of the middle ear cavity space (Voss et al. 2008, 2013), can greatly improve characterization of NMEP effects.

Unlike traditional 226 Hz tympanometry, WAI provides precise, wideband information about acoustic transmission in the presence of NMEP. The effects of NMEP on the absorbance level are relatively small when the NMEP is not extreme (e.g., −400 daPa, or no measureable TPP); in this study, a mean decrease of 2 dB in the region of maximum separation was observed, and the largest effects were about 5 dB. Such small changes are unlikely to significantly affect hearing thresholds, as observed by Rabinowitz (1981). However, other diagnostic measurements may be affected. For instance, DPOAE measurements (Sun & Shaver 2009; Thompson et al. 2015) rely on both forward and reverse transmission through the middle ear, which could double the level effect of NMEP. Note that WAI and OAEs are often measured using the same equipment, which may motivate the use of WAI to evaluate middle ear function in conjunction with OAE measurements.

One proposed method to circumvent the effects of NMEP on other measurements of hearing is to apply a compensatory pressure in the ear canal, and measure WAI and DPOAEs at the TPP (Sun & Shaver 2009; Shaver & Sun 2013). It is important to recognize that there may be subtle differences in middle ear transmission when using such methods. For instance, the results of Lynch et al. (1982), Lauxmann et al. (2014), and Myers et al. (1998) indicate that the difference between the middle and inner ear pressures may have an effect that is independent of the difference between the ear canal and middle ear pressures. Using ambient WAI, this experiment has demonstrated that it is possible for subjects to alter their middle ear pressure without reinsertion of the probe. Thus in some cases, if NMEP is suspected during a measurement sitting, the clinician or researcher could coach the subject to equalize their middle ear pressure, and then re-measure WAI.

Ambient WAI estimated at the TM provides a more accurate assessment of acoustic properties of the TM, without the flawed assumption (3) of tympanometry, over a much broader frequency range. In traditional WAI analysis, the effect of the REC is removed by considering only the power reflectance and absorbance level measured in the ear canal. Studies have shown that many properties of the middle ear can be analyzed using these magnitude-only quantities. In this study, we have estimated the phase response at the TM as well, which provides useful information regarding middle ear signal delay. Such delay information may help to pinpoint the source of disruption in middle ear sound transmission, via modeling. Refining this and similar methods of estimating the complex acoustic response at the TM should improve differential diagnosis of middle ear pathology, resulting in increased utility of WAI.

Summary

Our methods remove REC delay from the complex WAI, allowing for direct estimation of the complex WAI (magnitude and phase) at the TM. For the 8 subjects presented here, NMEP has the largest and most significant effect between 0.8 and 1.9 kHz, causing a mean reduction of 2 to 3 dB in energy absorbed by the middle ear and cochlea. However, WAI results vary considerably in magnitude and frequency range across ears. General changes in WAI at the TM due to NMEP, characterized by an increase in the TM impedance (decrease in the absorbance level) below 2 kHz, and a decrease at higher frequencies, appear consistent with previous results, and may be related to a stiffening of the tensor tympani, annular ligament, and other middle ear structures due to middle ear pressure.

Tympanometry, specifically the measurement of TPP, is the clinical gold standard for identifying ears compromised by middle ear pressure. However, TPP does not appear to be sufficiently related to wideband acoustic changes in the middle ear, quantified by the power absorbance level and estimated WAI at the TM, to be a reliable predictor of middle ear transmission in the presence of NMEP. WAI estimated at the TM is expected to be a better predictor of changes in wideband middle ear transmission due to NMEP. However, further experiments and analyses are needed to fully utilize WAI in this way.

ACKNOWLEDGMENTS

The authors are grateful to the reviewers and Judi Lapsley-Miller for valuable critique of this manuscript. The authors also appreciate the support of Glenis Long and Simon Henin in the Hearing Science lab at the CUNY Graduate Center, where the data for this study were collected.

Sarah Robinson was partially supported through a Research Assistantship funded by an STTR award from the Office of Naval Research under the contract number N00014-11-C-0498, and is a part-time employee of Mimosa Acoustics as of May 2015. Jont Allen is the CTO of Mimosa Acoustics, but is not a salaried employee of the company.

The authors have no conflicts of interest to disclose.

Address for correspondence: Sarah Robinson, University of Illinois, Urbana-Champaign, 2137 Beckman Institute MC 251, 405 N. Mathews Ave., Urbana, IL 61801, USA. E-mail: srrobin2@illinois.edu

Received February 13, 2015; accepted December 31, 2015.

REFERENCES

Allen, J. B. (1986). Measurements of eardrum acoustic impedance. In J. B. Allen, J. H. Hall, A. Hubbard, et al. (Eds.), *Peripheral Auditory Mechanisms* (pp. 44–51). New York, NY: Springer-Verlag.

Allen, J. B., Jeng, P. S., Levitt, H. (2005). Evaluation of human middle ear function via an acoustic power assessment. *J Rehabil Res Dev*, *42*(4 Suppl 2), 63–78.

Aron, M., Floyd, D., Bance, M. (2015). Voluntary eardrum movement: A marker for tensor tympani contraction? *Otol Neurotol*, *36*, 373–381.

Bance, M., Makki, F. M., Garland, P., et al. (2013). Effects of tensor tympani muscle contraction on the middle ear and markers of a contracted muscle. *Laryngoscope*, *123*, 1021–1027.

Bluestone, C. D. & Klein, J. O. (2007). *Otitis Media in Infants and Children* (pp. 42–64). Hamilton, Ontario, Canada: BC Decker Inc.

Eliachar, I., & Northern, J. L. (1974). Studies in tympanometry: Validation of the present technique for determining intra-tympanic pressures through the intact eardrum. *Laryngoscope*, *84*, 247–255.

Feeney, M. P., & Keefe, D. H. (1999). Acoustic reflex detection using wide-band acoustic reflectance, admittance, and power measurements. *J Speech Lang Hear Res*, *42*, 1029–1041.

Feeney, M. P., Grant, I. L., Marryott, L. P. (2003). Wideband energy reflectance measurements in adults with middle-ear disorders. *J Speech Lang Hear Res*, *46*, 901–911.

Feeney, M. P., Keefe, D. H., Sanford, C. A. (2004). Wideband reflectance measures of the ipsilateral acoustic stapedius reflex threshold. *Ear Hear*, *25*, 421–430.

Feeney, M. P., Hunter, L. L., Kei, J., et al. (2013). Consensus statement: Eriksholm workshop on wideband absorbance measures of the middle ear. *Ear Hear*, *34*(Suppl 1), 78S–79S.

Holmquist, J., & Olén, L. (1980). Evaluation of Eustachian tube function. *J Laryngol Otol*, *94*, 15–23.

Honjo, I., Kumazawa, T., Honda, K. (1981). Simple impedance test for Eustachian tube function. *Arch Otolaryngol*, *107*, 221–223.
Karal, F. (1953). The analogous acoustical impedance for discontinuities and constrictions of circular cross section. *J Acoust Soc Am*, *25*, 327–334.
Keefe, D. H. (1984). Acoustical wave propagation in cylindrical ducts: Transmission line parameter approximations for isothermal and nonisothermal boundary conditions. *J Acoust Soc Am*, *75*, 58–62.
Keefe, D. H., & Schairer, K. S. (2011). Specification of absorbed-sound power in the ear canal: Application to suppression of stimulus frequency otoacoustic emissions. *J Acoust Soc Am*, *129*, 779–791.
Keefe, D. H., Bulen, J. C., Arehart, K. H., et al. (1993). Ear-canal impedance and reflection coefficient in human infants and adults. *J Acoust Soc Am*, *94*, 2617–2638.
Kringlebotn, M. (1988). Network model for the human middle ear. *Scand Audiol*, *17*, 75–85.
Lauxmann, M., Eiber, A., Haag, F., et al. (2014). Nonlinear stiffness characteristics of the annular ligament. *J Acoust Soc Am*, *136*, 1756–1767.
Lynch, T. J. III, Nedzelnitsky, V., Peake, W. T. (1982). Input impedance of the cochlea in cat. *J Acoust Soc Am*, *72*, 108–130.
Marshall, L., Heller, L. M., Westhusin, L. J. (1997). Effect of negative middle-ear pressure on transient-evoked otoacoustic emissions. *Ear Hear*, *18*, 218–226.
Møller, A. R. (1960). Improved technique for detailed measurements of the middle ear impedance. *J Acoust Soc Am*, *32*(2), 250–257.
Møller, A. R. (1983). *Auditory Physiology*. New York, NY: Academic Press, Inc.
Monroy, G. L., Shelton, R. L., Nolan, R. M., et al. (2015). Noninvasive depth-resolved optical measurements of the tympanic membrane and middle ear for differentiating otitis media. *Laryngoscope*, *125*, E276–E282.
Mukerji, S., Windsor, A. M., Lee, D. J. (2010). Auditory brainstem circuits that mediate the middle ear muscle reflex. *Trends Amplif*, *14*, 170–191.
Murakami, S., Gyo, K., Goode, R. L. (1997). Effect of middle ear pressure change on middle ear mechanics. *Acta Otolaryngol*, *117*, 390–395.
Myers, E. N., Murakami, S., Gyo, K., et al. (1998). Effect of increased inner ear pressure on middle ear mechanics. *JAMA Otolaryngol Head Neck Surg*, *118*, 703–708.
Nakajima, H. H., Pisano, D. V., Roosli, C., et al. (2012). Comparison of ear-canal reflectance and umbo velocity in patients with conductive hearing loss: A preliminary study. *Ear Hear*, *33*, 35–43.
Nguyen, C. T., Jung, W., Kim, J., et al. (2012). Noninvasive *in vivo* optical detection of biofilm in the human middle ear. *Proc Natl Acad Sci USA*, *109*, 9529–9534.
Nguyen, C. T., Robinson, S. R., Jung, W., et al. (2013). Investigation of bacterial biofilm in the human middle ear using optical coherence tomography and acoustic measurements. *Hear Res*, *301*, 193–200.
Pang, X. D., & Peake, W. T. (1986). How do contractions of the stapedius muscle alter the acoustic properties of the ear? In J. B. Allen, J. H. Hall, A. Hubbard, et al. (Eds.), *Peripheral Auditory Mechanisms* (pp. 36–43). New York, NY: Springer-Verlag.
Parent, P., & Allen, J. B. (2010). Time-domain "wave" model of the human tympanic membrane. *Hear Res*, *263*, 152–167.
Prieve, B. A., Calandruccio, L., Fitzgerald, T., et al. (2008). Changes in transient-evoked otoacoustic emission levels with negative tympanometric peak pressure in infants and toddlers. *Ear Hear*, *29*, 533–542.
Prieve, B. A., Vander Werff, K. R., Preston, J. L., et al. (2013). Identification of conductive hearing loss in young infants using tympanometry and wideband reflectance. *Ear Hear*, *34*, 168–178.
Puria S. (1991). *A theory of cochlear input impedance and middle ear parameter estimation.* Doctoral dissertation, City University of New York.
Puria, S., & Allen, J. B. (1991). A parametric study of cochlear input impedance. *J Acoust Soc Am*, *89*, 287–309.
Puria, S., & Allen, J. B. (1998). Measurements and model of the cat middle ear: Evidence of tympanic membrane acoustic delay. *J Acoust Soc Am*, *104*, 3463–3481.
Rabinowitz, W. M. (1981). Measurement of the acoustic input immittance of the human ear. *J Acoust Soc Am*, *70*, 1025–1035.
Robinson, S. R., Nguyen, C. T., Allen, J. B. (2013). Characterizing the ear canal acoustic impedance and reflectance by pole-zero fitting. *Hear Res*, *301*, 168–182.
Rosowski, J. J., Nakajima, H. H., Hamade, M. A., et al. (2012). Ear-canal reflectance, umbo velocity, and tympanometry in normal-hearing adults. *Ear Hear*, *33*, 19–34.
Schairer, K. S., Ellison, J. C., Fitzpatrick, D., et al. (2007). Wideband ipsilateral measurements of middle-ear muscle reflex thresholds in children and adults. *J Acoust Soc Am*, *121*, 3607–3616.
Shahnaz, N., Bork, K., Polka, L., et al. (2009). Energy reflectance and tympanometry in normal and otosclerotic ears. *Ear Hear*, *30*, 219–233.
Shanks, J. E., & Lilly, D. J. (1981). An evaluation of tympanometric estimates of ear canal volume. *J Speech Hear Res*, *24*, 557–566.
Shanks, J., & Shohet, J. (2009). Tympanometry in clinical practice. In J. Katz, L. Medwetsky, R. Burkard, et al. (Eds.), *Handbook of Clinical Audiology* (pp. 157–188). Baltimore, MD: LWW.
Shanks, J. E., Lilly, D. J., R. Margolis, H., et al. (1988). Tympanometry. *J Speech Hear Disord*, *53*, 354–377.
Shaver, M. D., & Sun, X. M. (2013). Wideband energy reflectance measurements: Effects of negative middle ear pressure and application of a pressure compensation procedure. *J Acoust Soc Am*, *134*, 332–341.
Sun, X. M., & Shaver, M. D. (2009). Effects of negative middle ear pressure on distortion product otoacoustic emissions and application of a compensation procedure in humans. *Ear Hear*, *30*, 191–202.
Thompson, S., Henin, S., Long, G. R. (2015). Negative middle ear pressure and composite and component distortion product otoacoustic emissions. *Ear Hear*, *36*, 695–704.
Tideholm, B., Carlborg, B., Jönsson, S., et al. (1998). Continuous long-term measurements of the middle ear pressure in subjects without a history of ear disease. *Acta Otolaryngol*, *118*, 369–374.
Vanhuyse, V. J., Creten, W. L., Van Camp, K. J. (1975). On the w-notching of tympanograms. *Scand Audiol*, *4*, 45–50.
Voss, S. E., & Allen, J. B. (1994). Measurement of acoustic impedance and reflectance in the human ear canal. *J Acoust Soc Am*, *95*, 372–384.
Voss, S. E., Merchant, G. R., Horton, N. J. (2012). Effects of middle-ear disorders on power reflectance measured in cadaveric ear canals. *Ear Hear*, *33*, 195–208.
Voss, S. E., Horton, N. J., Woodbury, R. R., et al. (2008). Sources of variability in reflectance measurements on normal cadaver ears. *Ear Hear*, *29*, 651–665.
Voss, S. E., Stenfelt, S., Neely, S. T., et al. (2013). Factors that introduce intrasubject variability into ear-canal absorbance measurements. *Ear Hear*, *34*(Suppl 1), 60S–64S.
Zwislocki, J. (1962). Analysis of the middle-ear function. Part I: Input impedance. *J Acoust Soc Am*, *34*, 1514–1523.